8th Int. Symp. "Nanostructures: Physics and Technology"
St Petersburg, Russia, June 19–23, 2000

Charge separation in scrolled heterostructures

V. M. Osadchii and V. Ya. Prinz
Institute of Semiconductor Physics, 630090, Novosibirsk, Russia

Abstract. We calculate strains in the wall of semiconductor InAs/GaAs nanotube and their effects on the band edges. We show that the maxima of the electron and hole wave functions are shifted in opposite directions from the middle of the tube wall.

Recently, self-formed semiconductor nanotubes have been fabricated, and the possibility of precise control over their parameters has been shown [1, 2]. In the fabrication process, highly strained InGaAs/GaAs heterolayers are used, which, after being debonded from substrate (by selective etching of an underlying AlAs sacrificial layer), roll up in scrolls. The rolled up layers in the resultant tube were shown to perfectly stick together, thus forming a monocrystalline tube wall. It is the electrical and optical properties of these structures that are of primary interest.

Properties of a 2D electron gas on a cylindrical surface were theoretically considered in [3–5]. However, in addition to pure bending, notable strains take place in real structures, which should also be factors affecting the energy spectrum of electrons in nanotubes. In this work, within a simple model, strains in the wall of a nanotube scrolled up from a GaAs/InAs bilayer film MBE-grown on an InP substrate are calculated, as well as energy levels and wave functions of charge carriers.

The heterostructure GaAs/InAs is strained because of the mismatch of lattice parameters of two layers $f = \Delta a/a$ ($\approx$7%), the GaAs and InAs layers being in tension and in compression, respectively. After the bilayer film is freed from bonding with substrate, the elastic stresses are relaxed, and the film scrolls up in a tube. Provided that the layers in the tube stick together in a coherent manner, as their number increases, the outer layers of the tube becomes more and more stretched, while the tension in the inner layers also grows in value. Figure 1(a) shows the structure under consideration. Here, we assume that the tube is axially symmetrical, its elastic constants do not depend on crystallographic direction, the initial film is grown on a (100) substrate, and the axis of the tube is directed along the[010] axis. Under these conditions, only diagonal components of the strain tensor appear to be non-zero, the axial, azimuth, and radial strains being designated as ε_z, ε_θ and ε_r. Inner radius R of tube is determined as a curvature radius of bilayer film [6]. We calculate the strains using the continuum elasticity theory, since this theory proved to be applicable at least to films as thick as 3 ML [7].

The axial strain ε_z can be calculated as follows. It is apparent that the lattice parameter a_z in the direction along the tube axis is equal to that in a free-standing planar superlattice with two alternate layers [8]:

$$a_z = \frac{a_1 G_1 h_1 + a_2 G_2 h_2}{G_1 h_1 + G_2 h_2},$$

where, for each layer, h_i is the layer thickness ($i = 1, 2$), $G_i = E_i/(1-\nu_i)$, E_i is the Young modulus, ν_i is the Poisson ratio, and a_i is the lattice parameter. The difference in the lattice

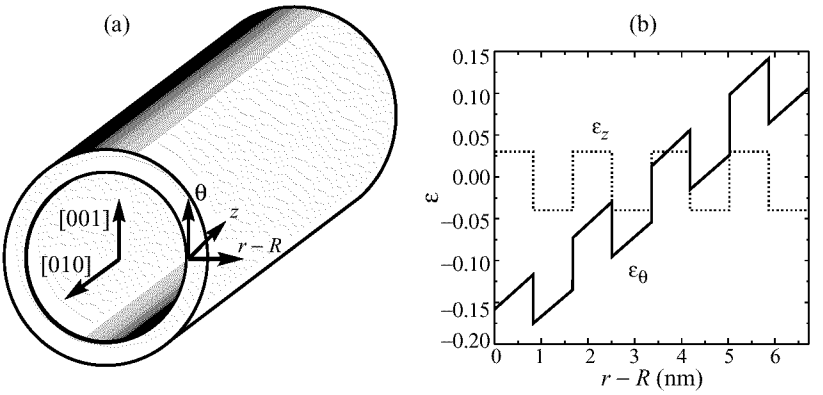

Fig. 1. (a) Schematic view of nanotube. Direction (z, θ, r) for the calculation of strain tensor components are shown. R is inside radius of tube. (b) Azimuth ε_θ and axial ε_z components of strain tensor across the tube wall (4 bilayers 3 ML GaAs/3 ML InAs).

parameter of the bulk material and strained structure determines the strain $\varepsilon_z = (a_i - a_z)/a_z$ (Fig. 1(b), curve 1). The calculations are performed for the 4 turn tube with thicknesses of InAs and GaAs layers of 3 ML. For GaAs $a = 0.5653$ nm, $E = 85.5$ GPa, and $\nu = 0.31$, while for InAs $a = 0.6058$ nm, $E = 51.4$ GPa, and $\nu = 0.35$.

In calculating the azimuth strain, we assumed that the neutral surface (the boundary between the layers in tension and in compression) passes inside the tube wall. The lattice parameter a_θ in the azimuth direction equals a_z: under this condition, as our estimates showed, the energy of the elastic deformation is nearly minimal. It is apparent that, for a single-crystal tube, a_θ varies linearly in the radial direction (Fig. 1(b), curve 2). From the known strains in two directions, the strain in the radial direction can be readily found from the Poisson relation $\varepsilon_r = -(\nu/1 - \nu)(\varepsilon_\theta + \varepsilon_z)$.

The strain shift band edges in a semiconductor [8]: the shift of the conduction band is $\Delta E_c = a_c Tr(\varepsilon)$ and that of the valence band is

$$\Delta E_{hh_l h} = a_v Tr(\varepsilon) \mp b\left(\varepsilon_r - \frac{\varepsilon_\theta + \varepsilon_z}{2}\right)$$

(here the upper and lower signs correspond to the band of heavy and light holes, respectively), where $Tr(\varepsilon) = \varepsilon_r + \varepsilon_\theta + \varepsilon_z$, and a_c, a_v, and b are the deformation potentials. In GaAs $a_c = -7.17$ eV, $a_v = 1.16$ eV, $b = -1.6$ eV, and in InAs $a_c = -5.08$ eV, $a_v = 1$ eV, $b = -1.6$ eV. Since the off-diagonal components of the strain tensor equal zero, the piezoelectric field equals zero too [9]. The calculated profiles of the band edges (those of the condition band and the valence band for heavy holes) across the tube wall in the non-doped structure are shown in Fig. 2(a) (solid curves). Here, the fact that the bandgaps in GaAs and in InAs are $E_g = 1.424$ and 0.355 eV and the electron affinities are $\chi = 4.07$ and 4.9 eV, respectively, is taken into account. As is seen, there is a modulation of the bandgap in the structure, the bandgap in each layer and the edges of both bands decreasing toward the outer surface of the tube wall. It should be noted that the near-surface bending of energy bands, in view of its being small in non-doped structures, was ignored.

From the known spatial profile of band edges, we can find the energy spectrum and wave functions of charge carriers in the structure of interest. We restrict our consideration to the ground state for electron and holes. The Schrödinger equation in the effective-mass

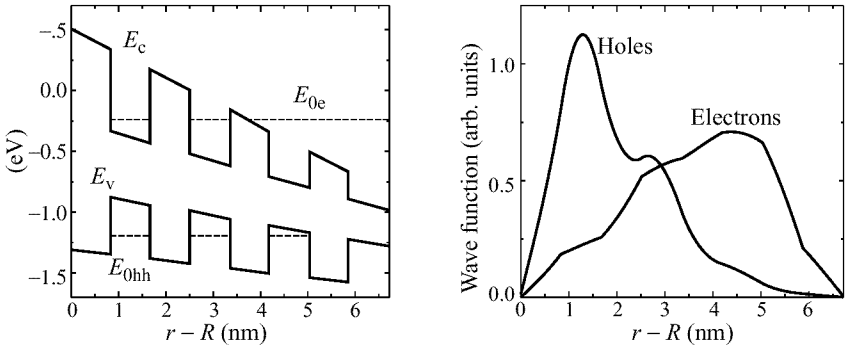

Fig. 2. (a) Conduction (E_c) and valence (E_v) band edges across the tube wall, and electron (E_{0e}) and hole (E_{0hh}) energy levels. (b) Wave functions across the tube wall.

approximation for the radial part of the wave function of the ground state Ψ is

$$-\frac{\hbar^2}{2m^*}\frac{1}{r}\frac{\mathrm{d}}{\mathrm{d}r}\left(r\frac{\mathrm{d}\Psi}{\mathrm{d}r}\right)+U\Psi=E_0\Psi. \tag{1}$$

Here m^* is the effective electron (hole) mass and U is the potential energy (edges of the corresponding band). The electron mass was assumed to equal $m^* = 0.067m_0$ and $0.023m_0$ in GaAs and in InAs, respectively, where m_0 is the free electron mass, the hole mass in both materials being equal to $0.4m_0$. The single-band effective mass approximation is known to be capable of adequate reproducing the energy levels for electron and holes in their ground states [10], whereas, for the excited states of holes, mixing of states of heavy and light holes should be necessarily taken into account. The adopted boundary conditions for the wave function were its zero value at the tube-wall surfaces and the continuity of Ψ and $1/m^*\mathrm{d}\Psi/\mathrm{d}r$ at heterointerfaces.

Since, in the Schrödinger equation, the potential energy for the structure of interest is a piecewise continuous function of the coordinate, the solution of the equation in this case cannot be expressed in terms of analytical functions and should be found numerically. In Figure 2(a), the dotted curves show the calculated energy levels of electrons and holes. Here, the electron level for the state in the Γ-minimum is shown. The effective masses in the subsidiary (L and X) minima are greater than that in the Γ-minimum, and the spatial-quantization levels here rise more slowly with decreasing dimensions of the well. However, calculation shows that the Γ-valley electron state is the ground one for the tubes with InAs layers being thicker than one monolayer, which is also the case for the free-standing GaAs/InAs superlattices [11].

Figure 2(b) shows the calculated wave functions for electrons and holes. An appreciable spatial redistribution of holes and electrons is seen to take place, which could be expected beforehand from the profiles of bend edges (Fig. 2(a)). As calculations showed, the spatial separation of charge carriers is observed in the cases where the number of rolls in the tube exceeds 2, and the degree of the charge redistribution increases with increasing number of rolls.

Now we shall dwell briefly on the magnitude of strain in tube walls (Fig. 1(b)). As is seen from the figure, the highest strain here far exceeds the strain attainable in pseudomorphic MBE-grown layers. It is possible to grow 4 ML GaAs and 4 ML InAs layers on an InP substrate, with the strain at the interface between layers being about 4%. In Fig. 1(b), the

two bilayers in the middle of the tube wall suffer a comparable strain. However, the strain in outer layers runs into 12%. At growth temperatures, such a strain would give rise to dislocations. However, in the case under study we have already formed pseudomorphic initial film, which roll up in the tube at room temperature, no dislocations being introduced here, which is confirmed by a HREM study [2] of similar tube.

Acknowledgements

Authors thank Dr. R. M. Taziev for helpful discussions. This work was supported by the Russian Foundation for Basic Research (Grants 00-02-16764, 99-02-16689) and Russian Program "Physics of Solid State Nanostructures" (Project 98-2030).

References

[1] V. Ya. Prinz, V. A. Seleznev and A. K. Gutakovsky, *Proc. ICPS-24 (Jerusalem 1998)* World Scientific (1999).

[2] V. Ya. Prinz, V. A. Seleznev, A. K. Gutakovsky, A. V. Chehovskiy, V. V. Preobrazhenskii, M. A. Putyato and T. A. Gavrilova, *Physica E* **6**, 828 (2000).

[3] L. I. Magarill, D. A. Romanov and A. V. Chaplik, *ZhETF* **113**, 1411 (1998).

[4] L. I. Magarill and A. V. Chaplik, *ZhETF* **115**, 1478 (1999)

[5] V. A. Geiler, V. A. Margulis and A. V. Shorokhov, *ZhETF* **115**, 1450 (1999).

[6] Y. C. Tsui and T. W. Clyne, *Thin Solid Films* **306**, 23 (1997).

[7] O. Brandt, K. Ploog, R. Bierwolf and M. Hohenstein, *Phys. Rev. Lett.* **68**, 1339 (1992).

[8] C. G. Van de Walle, *Phys. Rev. B* **39**, 1871 (1989).

[9] L. De Caro and L. Tapfer, *Phys. Rev. B* **51**, 4381 (1995).

[10] H. Jiang and J. Singh, *Phys. Rev. B* **56**, 4696 (1997).

[11] A. Taguchi and T. Ohno, *Phys. Rev. B* **38**, 2038 (1988).